Grain Shape and Size and Structural and Phase Conditions Modified by Aluminum Ion Implantation in UFG Titanium

Alisa Nikonenko[1,a)], Natalya Popova[2,3,b)], Elena Nikonenko[2,4,c)], Mark Kalashnikov[3,4,d)], Irina Kurzina[1,e)]

[1]*National Research Tomsk State University, 36 Lenina Avenue, Tomsk 634050, Russian Federation*
[2]*Tomsk State University of Architecture and Building, 2 Solyanaya Square, Tomsk 634003, Russian Federation*
[3]*Institute of Strength Physics and Materials Science, SB RAS, 2/1 Akademichesky Avenue, Tomsk 634021, Russian Federation*
[4]*National Research Tomsk Polytechnic University, 30 Lenina Avenue, Tomsk 634050, Russian Federation*

[a)]corresponding author: aliska-nik@mail.ru
[b)]natalya-popova-44@mail.ru
[c)]vilatomsk@mail.ru
[d)]kmp1980@mail.ru
[e)]kurzina99@mail.ru

Abstract. The paper presents the transmission electron microscopy investigations of the granular state and the structural and phase conditions of commercially pure ultra-fine grain (UFG) titanium VT1-0 alloyed with aluminum ions. The UFG-titanium is obtained by the multiple uniaxial compaction with intermediate annealing. The ion implantation is carried out on Mevva-V.Ru ion source at ion-implantation dosages of $1\cdot10^{17}$, $5\cdot10^{17}$ and $1\cdot10^{18}$ ion/cm^2. The functions are constructed for the grain size distribution in longitudinal and cross sections; the average grain size and the grain anisotropy factor are determined in this paper. It is shown that the grain shape and size of titanium specimens are modified due to the ion implantation. With the increase of the ion-implantation dosage the anisotropy factor decreases three times. At $1\cdot10^{18}$ ion/cm^2 ion-implantation dosage the longitudinal grain size comes to 0.7 μm. The phase composition of the alloy is detected after the ion implantation and its modification induced by the implantation dosage. The quantitative characteristics and locations of secondary β-Ti, $TiAl_3$, Ti_3Al, TiC and TiO_2 phases are ascertained during the investigations. It is shown that $TiAl_3$ and Ti_3Al are ordered phases formed during the ion implantation on α-Ti grain boundaries. The volume ratios of these phases are detected and determined by the ion-implantation dosage. The volume ratios of α-Ti and secondary TiC and TiO_2 phases do not depend on the implantation dosage and range between 0.3–0.9 vol.%.

INTRODUCTION

Presently methods of the modification materials by ion beams are the most rapidly developing areas of the new materials synthesis [1-3]. It has to be noted that mostly experimental data of modification by ion beam obtained on the materials in polycrystalline or macrocrystalline state [1-3]. However, reducing the grain size of the target can lead to a sharp acceleration of diffusion processes, alloying, stirring, formation of secondary phases and defects [3], as well as the formation of the new, phase including thermodynamically unstable phases [4].The industrial applications of ultra-fine grain (UFG) titanium are conditioned by a favorable combination of its mechanical strength, corrosion and heat resistance and low density [5]. Titanium produced by the severe plastic deformation holds a special place among UFG materials [6, 7]. UFG titanium possesses a complex microstructure and specific properties such as a small grain size (sub-micro- and nanoscale), low density of free dislocations, large-angle grain boundaries, non-equilibrium boundary conditions.

The service characteristics of UFG titanium can be considerably improved by its surface modification [6]. The problems connected with the synthesis of nanocrystal secondary phases and the structural modification

Prospects of Fundamental Sciences Development (PFSD-2016)
AIP Conf. Proc. 1772, 030007-1–030007-7; doi: 10.1063/1.4964545
Published by AIP Publishing. 978-0-7354-1430-3/$30.00

of UFG titanium surface layers, are still being solved. Also, the effect from the ion-implantation dosage on the grain structure and phase composition of UFG titanium has not yet clarified.

The aim of this work is to analyze the grain structure and phase composition of UFG titanium before and after the aluminum ion implantation performed using the different dosages, namely: $1\cdot10^{17}$, $5\cdot10^{17}$ and $1\cdot10^{18}$ ion/cm^2.

MATERIALS AND METHODS

The type VT1-0 titanium was used as the original material for the implantation with aluminum ions. The formation of the ultra-fine grain (UFG) state of titanium specimens was provided by the triple uniaxial compaction with intermediate annealing. The temperature of compaction was constant during each cycle, however decreased stage-by-stage during the transition from preceded compaction to the next one within the temperature range of 500 –400 K. The rate of deformation during the uniaxial compaction ranged from 10^{-2} to 10^{-1} s^{-1}. The degree of deformation at single uniaxial compaction came to 40-50 %. The specimen was turned through 90° at each compaction. The value of cumulative deformation was 2.12. After the compaction stage, the Ti specimen was deformed by multipass rolling in grooved rolls at room temperature, the value of cumulative deformation being 75 %. After the multipass rolling, Ti specimens took the form of 6 mm square bars and 500 mm length. The rolled Ti bars were annealed at 573 K to improve their plasticity. The annealing did not modify the structural state of the alloy but increased its tensile ductility up to 6–8 %.

The ion implantation of titanium specimens was carried out on Mevva-V.Ru ion source [8] at 623 K temperature; 50 kV accelerating voltage; 6.5 mA/cm^2 ion beam density; 60 cm distance from the ion-optical system. The variation of the ion-implantation dosages ($1\cdot10^{17}$, $5\cdot10^{17}$ and $1\cdot10^{18}$ ion/cm^2) was achieved due to the variable time of implantation (0.5 h; 3 h; 5.25 h). The chemical composition of the implanted material was analyzed on Auger electron spectrometer 90IOS [9]. The grain structure of titanium was investigated on the transmission electron microscope (TEM) EM-125K at 120 kV accelerating voltage. The modified layer of implanted specimens was investigated at a depth of 50–70 nm from the implanted surface.

RESULTS AND DISCUSSION

The experiments show that strongly elongated elements (grains) having the well-defined texture, are present in the UFG titanium before the ion implantation. TEM image of the fine grain structure is shown in Fig. 1a.

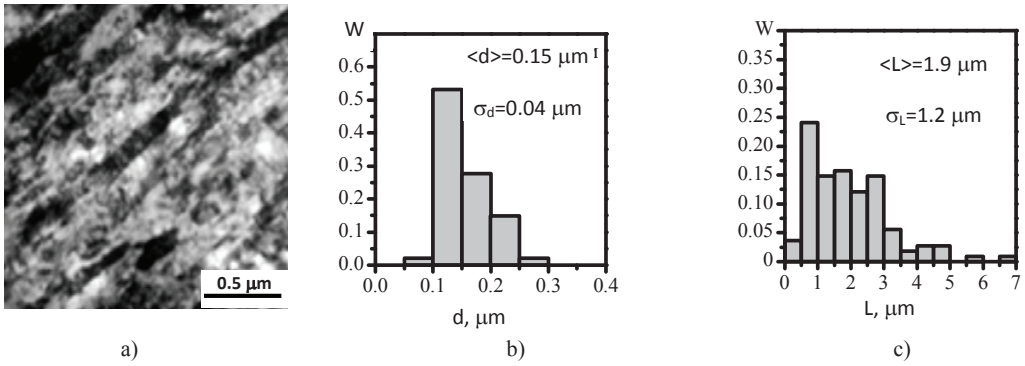

FIGURE 1. TEM images (a) and grain size distribution: b – crosswise d, c – longitudinal L to ion implantation

The analysis of grain sizes shows that their crosswise size ranges between 0.05–0.30 μm (Fig. 1b). The grains having less than 0.2 μm occupy some 75 % of the volume. The distribution function is unimodal. Its average size is $\langle d\rangle = 0.15\pm0.02$ μm. The maximum of the unimodal distribution function is within the average value. The longitudinal grain size ranges between 0.1–7.0 μm. The distribution function is also unimodal with the maximum within the average value. The average longitudinal grain size is $\langle L\rangle = 1.9 \pm 0.6$ μm. The grain anisotropy factor is $K = L/d = 12.7$. In fact, the method of specimen preparation leads to the formation of the stripe fragmented structure. And the non-uniform diffraction contrast inside grains and the diffuse interface shown in Fig. 1 a, indicate to the high internal stresses and high scalar density of dislocations.

As a result of ion implantation, a significant modification of grain size and shape is observed in UFG titanium. Figure 2 demonstrates TEM images of the grain structure and size distribution observed at different dosages of ion implantation.

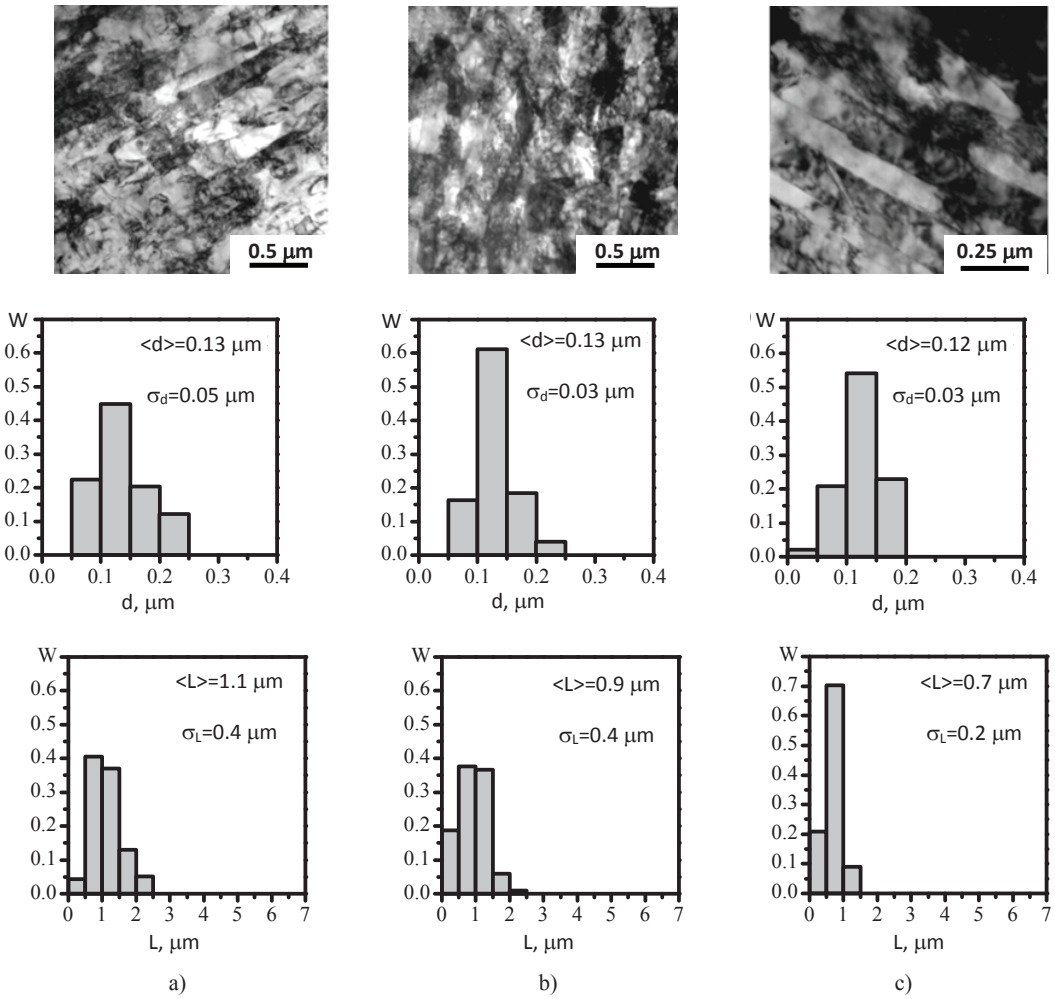

FIGURE 2. TEM images and grain size distribution (d – crosswise and L – longitudinal) in UFG titanium after ion implantation dosages: a – $1 \cdot 10^{17}$, b – $5 \cdot 10^{17}$, c – $10 \cdot 10^{17}$ ion/cm.

According to this Figure, $1 \cdot 10^{17}$ ion/cm^2 ion-implantation dosage results in the insignificant reduction of the crosswise grain size, i.e. $\langle d \rangle = 0.13 \pm 0.02$ μm. However, the distribution function has changed. Thus, before the ion implantation the crosswise grain size ranges within 0.05–0.30 μm, while after the ion implantation it ranges within 0.05–0.25 μm. Herewith, the amount of fine grains is 0.05–0.10 μm, i.e. 20 %, while before the implantation it does not exceed 3 %. The amount of coarse grains ranges within 0.20–0.25 μm, i.e. decreases down to 15 %. It is worth noting that before ion implantation, the amount of 0.20–0.30 μm coarse grains is 20 %. Nevertheless, the distribution function of crosswise grains is still unimodal with the maximum within the average values.

After the ion implantation, the longitudinal grain size is modified rather significantly and is averagely 1.1 μm. The dispersion also decreases (σ_L = 0.4 μm). The type of the distribution function is changed also. Thus, before the implantation the longitudinal grain size ranges from 0.1 to 7.0 μm, while after the implantation it reduces to 0.1–2.5 μm. The distribution function is unimodal with the maximum within the average value.

Thus, the titanium implantation with aluminum ions results in the refinement of its grain structure. The increase of the implantation dosage results to the subsequent decrease in the grain size, and at the maximum implantation dosage the average values are 0.12 and 0.70 μm for the crosswise and longitudinal size respectively. According to the diagrams shown in Fig. 2, the types of functions for the both crosswise and longitudinal grain sizes are changed. More and more fine grains are observed in titanium rather than grains having a large size. The distribution functions of the both crosswise and longitudinal sizes stay unimodal. The maximums of functions are still within the average values.

As shown in Figure 3, the anisotropy factor *K* decreases with the increase of the ion-implantation dosage. In comparison with the original state of titanium, i.e. before the ion implantation, E = 0, the decrease of the anisotropy factor is rather considerable at E = $1 \cdot 10^{17}$ ion/cm^2 (*K* = 8.5). And at the increase of the implantation dosage, the anisotropy factor *K* decreases insignificantly.

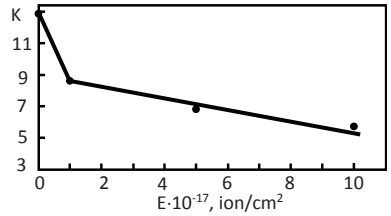

FIGURE 3. Dependence between anisotropy factor and implantation dosage

TEM investigations show that the phase composition of VT1-0 alloy in its original state involves β-Ti phase along with α-Ti phase having the hexagonal close-packed (HCP) crystal system (*P6$_3$/mmc* space group). β-Ti phase has the body-centered cubic (BCC) crystal system (*Im3m* space group). The particles of this phase are represented by laminae parallel to each other and located inside α-Ti phase. The average width and length of some laminae in α-Ti phase come to 70 and 200 nm, respectively. The formation of β-Ti phase occurs under the severe plastic deformation and the subsequent annealing at 573 K during the transformation of α-Ti → β-Ti. The volume ratio is not large, namely 0.9 vol. %.

The aluminum ion implantation of VT1-0 alloy modies its phase composition. As before, the lamellar β-Ti precipitates are present inside α-Ti grains (Fig. 4). The increase in the ion-implantation dosage *E* results in decrease of the lamina sizes in β-Ti phase (Fig. 5 a). However, its volume ratio is not changed (Fig. 6).

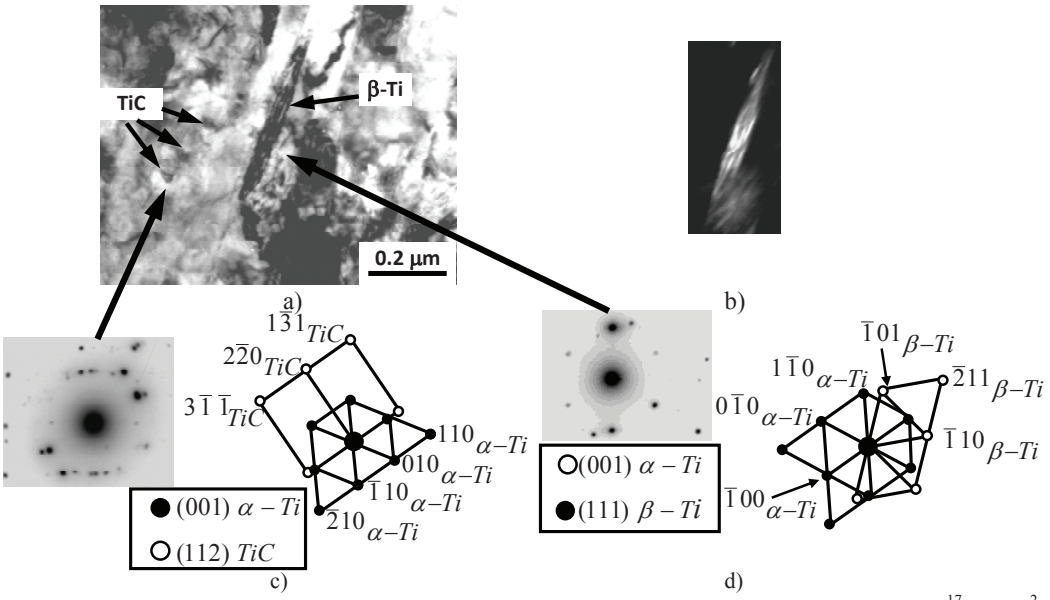

FIGURE 4. TEM images of particle precipitation in β-Ti and TiC phases inside α-Ti grains at $1 \cdot 10^{17}$ ion/cm^2 implantation dosage: *a* – bright-field image; *b* – dark-field image obtained in $[\bar{1}01]$ reflection of β-Ti phase; *c, d* – micro-diffraction patterns obtained from areas indicated by arrows (*a*)*; e, f* – their visual displays.

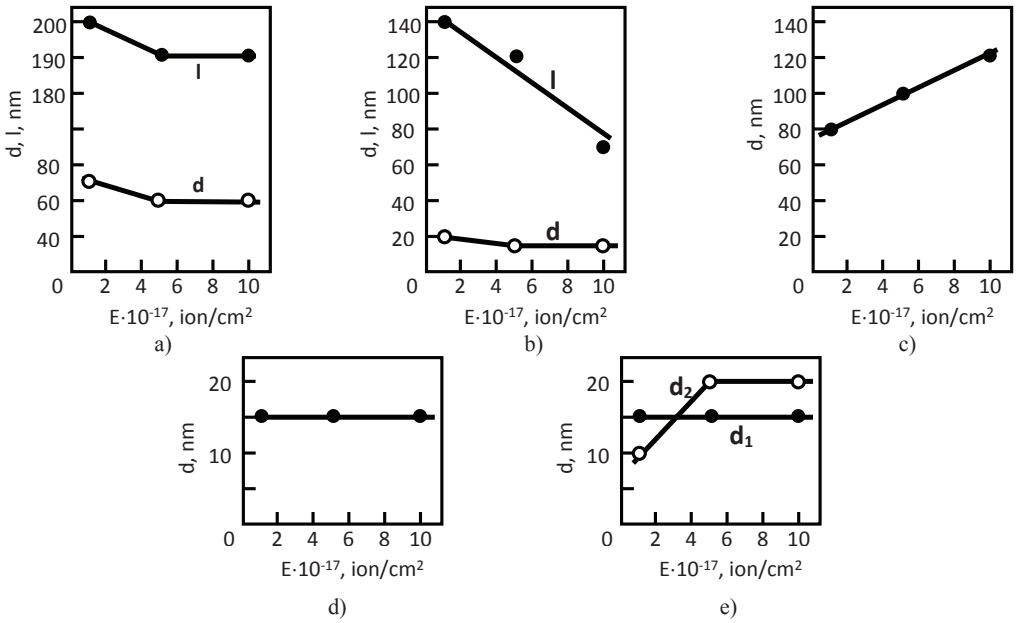

FIGURE 5. Diagrams of ion-implantation dosage E depending on phase particle size: *a* – β-Ti (*l* – longitudinal, *d* –crosswise); *b* – Ti_3Al (*l* – longitudinal, *d* – crosswise); *c* – $TiAl_3$ (diameter *d*); *d* – TiC (diameter *d*); *e* – TiO_2 (d_1 – inside grains, d_2 – on grain boundaries.)

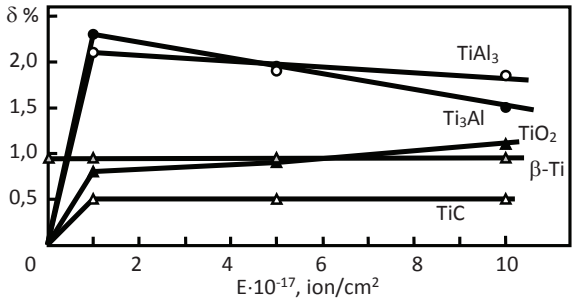

FIGURE 6. Dependence between ion-implantation dosage and volume ratios of secondary phases

The ion implantation results in the formation of new phases, namely Ti_3Al, $TiAl_3$, TiC and TiO_2. Ti_3Al phase shown in Fig. 7, is an ordered phase having $D0_{19}$ superstructure and HCP crystal system (*P6₃/mmc* space group). The particles of this phase have the form of laminae and are located along α-Ti grain boundaries.

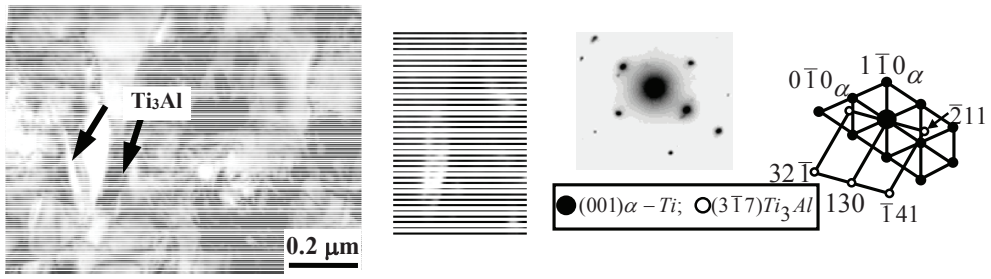

FIGURE 7. TEM images of lamellar Ti_3Al phase along α-Ti grain boundaries at $1 \cdot 10^{17}$ ion/cm^2 implantation dosage: *a* – bright-field image, *b* – dark-field image obtained in $\bar{2}11$ reflection of Ti_3Al phase; *c* – micro-diffraction pattern and its visual display

With the increase of the ion-implantation dosage E, the particle size decreases (see Fig. 5 b). Unlike the crosswise size, the most notable decrease is observed in the longitudinal size. The volume ratio of Ti_3Al phase particles also decreases (see Fig. 6). This behavior of phase particles is, obviously, connected with TEM

investigations carried out nearby the specimen surface, where the aluminum concentration is not over 30-40 at.% for $1–5\cdot10^{17}$ ion/cm^2 and 10 at.% for 10^{18} ion/cm^2 dosages [5].

The ordered Ti_3Al phase has $D0_{19}$ superstructure (*I4/mmm* space group) and the body-centered tetragonal (BCT) crystal system. Ti_3Al phase particles are mostly rounded and located in the boundary intersections and grain boundaries of α-Ti phase (Fig. 8). The average particle size increases with the increase of the ion-implantation dosage (see Fig. 5 c). The volume ratio of this phase is practically unchanged (Fig. 6). According to the phase diagram described by Lyakishev [10], Ti_3Al phase is formed at 50 at.% aluminum concentrations. The formation of this phase was earlier observed in the work of Kurzina *et al.* [4] in fine-grain materials with high defectiveness resulted from the diffusion processes in aluminum ions.

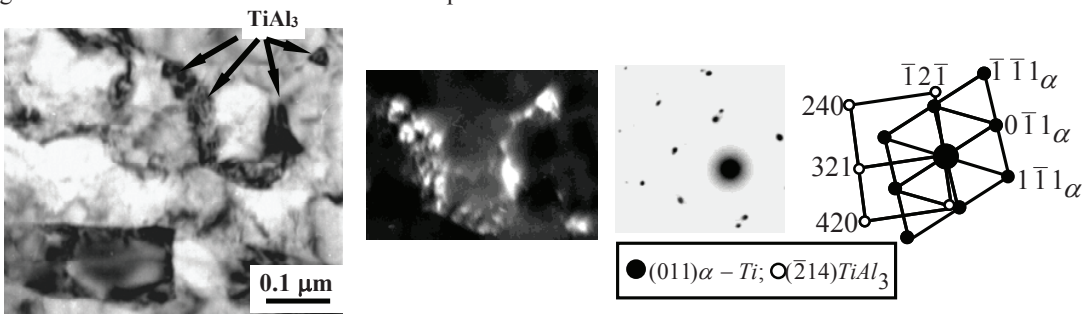

a) b) c)

FIGURE 8. TEM images of rounded Ti_3Al phase in the boundary intersections and grain boundaries of α-Ti phase at α-Ti at $1\cdot10^{17}$ ion/cm^2 implantation dosage: *a* – bright-field image, *b* – dark-field image obtained in $\bar{1}2\bar{1}$ reflection of Ti_3Al phase; *c* – micro-diffraction pattern and its visual display

TiC phase has the face-centered cubic (FCC) crystal system (*Fm3m* space group). TiC particles are observed on the dislocations inside α-Ti grains (see Fig. 4) and possess a rounded shape. According to Fig. 5d and 56, the increase in the ion implantation does not lead to the modification of the particle size and their volume ratio.

TiO_2 phase (brookite) possesses the orthorhombic crystal system (*Pbca* space group). TiO_2 phase particles are rounded and located on the dislocations inside α-Ti grains and their boundaries (Fig. 9). The increase of the ion-implantation dosage has no effect on the particle size located on the dislocations (Fig. 5e), however, it leads to a certain increase of their volume ratio (Fig. 6). The size of particles located on α-Ti grain boundaries increases with the increase of the implantation dosage (Fig. 5e), but their volume ratio is unchanged (Fig. 6).

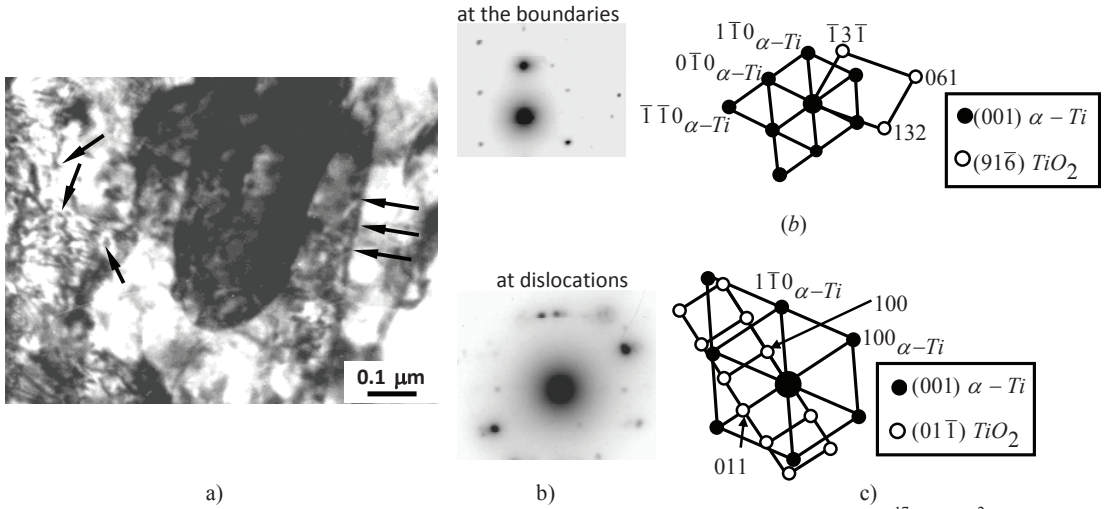

a) b) c)

FIGURE 9. TEM images of rounded TiO_2 phase inside α-Ti grains and their boundaries at $1\cdot10^{17}$ ion/cm^2 implantation dosage: *a* – bright-field image, *b, c*– micro-diffraction patterns and their visual displays

CONCLUSION

TEM investigations showed that the aluminum-ion implantation of titanium resulted, firstly, in the decrease of the anisotropy factor; secondly, in greater isotropy of grains with the increase of the implantation

dosage and, thirdly, the formation of a polyphase implanted layer based on α-Ti grains and comprising aluminide (Ti_3Al, $TiAl_3$), oxide (TiO_2) and carbide (TiC) phases. Ti_3Al particles were lamellar and located on the grain boundaries, while $TiAl_3$ particles were rounded and located in triple boundary intersections and grain boundaries. The volume ratio of Ti_3Al and $TiAl_3$ phases was defined by the implantation dosage. The concentration of oxide and carbide phases did not depend on the ion-implantation. The significant structural modification was primarily connected with the energy effect under the ion-implantation conditions. Since the increase of the implantation dosage depended on the increase of its duration, the titanium modification occurred due to both the energy effect and the local temperature increase during the ion implantation.

ACKNOWLEDGEMENT

This work was financially supported by Grants N 3.295.2014/K, N 461 from the Ministry of Education and Science of the Russian Federation and Grant N 16-48-700198/16 from the Russian Foundation for Basic Research.

REFERENCES

1. G. Brown, Nucl. Instr. Meth. **B37/38**, 68–73 (1989).
2. I. Tsiganov, E. Wieser, W. Matz, A. Mücklich, H. Reuther, M. T. Pham and E. Richter, Thin Solid Films. **376**, 188–197 (2000).
3. V. A. Gribkov, F. I. Grigor'yev and B. A. Kalin, *Perspective radiation beam technologies of processing of materials* (Izd. dom «Kruglyy god», Moscow, 2001) (in Russian) 528 p.
4. I. A. Kurzina, N. A. Popova, E. L. Nikonenko, M. P. Kalashnikov, K. P. Savkin, Yu. P. Sharkeev and E. V. Kozlov, B. Russ. Acad. Sci.: Physics **76, 1,** 64–68 (2012).
5. Yu. P. Sharkeev, A. Yu. Eroshenko, A. D. Bratchikov, E. V. Legostaeva and V. A. Kukareko, Phys. Mesomech. (Fizicheskaya Mezomekhanika – in Russian) **91, 8** 91–94 (2005).
6. I. A. Kurzina, E. V. Kozlov and Yu. P. Sharkeev, *Gradient surface layers based on intermetallic particles: synthesis, structure, properties* (NTL Publ., Tomsk, 2013) (in Russian) 260p.
7. A. Yu. Eroshenko, Yu. P. Sharkeev, A. I. Tolmachev, G. L. Korobitsyn and V. I. Danilov, J. Adv. Mater. (Zhurnal perspektivnye materialy – in Russian) **7** 107-112 **(**2009).
8. K. P. Savkin, A. G. Nikolaev, E. M. Oks and G. Yu. Yushkov, "Ion beam mass and charge composition for the vacuum arc Mevva-V.RU metal ion source with compound cathodes" in Proc. 9th Int. Conf. on Modification of Materials with Particle Beams and Plasma Flows. (TPU Publ., Tomsk, 2008) pp.68-71.
9. I. A. Kurzina, N. A. Popova, E. L. Nikonenko, M. P. Kalashnikov and E. V. Kozlov, B. Russ. Acad. Sci.: Physics, **77, 11** 1669-1672 (2013).
10. N. P. Lyakishev, *Phase diagrams of binary metal systems* (Mashinostroenie, Moscow, 1996) (in Russian) 992 p.